LAWRENCE
LIVERMORE
NATIONAL
LABORATORY

Model verification: synthetic single pattern simulations using seismic reflection data

A. Ramirez, K. Dyer, D. White, Y. Hao, X. Yang

July 12, 2010

Disclaimer

This document was prepared as an account of work sponsored by an agency of the United States government. Neither the United States government nor Lawrence Livermore National Security, LLC, nor any of their employees makes any warranty, expressed or implied, or assumes any legal liability or responsibility for the accuracy, completeness, or usefulness of any information, apparatus, product, or process disclosed, or represents that its use would not infringe privately owned rights. Reference herein to any specific commercial product, process, or service by trade name, trademark, manufacturer, or otherwise does not necessarily constitute or imply its endorsement, recommendation, or favoring by the United States government or Lawrence Livermore National Security, LLC. The views and opinions of authors expressed herein do not necessarily state or reflect those of the United States government or Lawrence Livermore National Security, LLC, and shall not be used for advertising or product endorsement purposes.

Theme 3B: Storage Monitoring Methods
Task 3b.11: Forward-Tuned Stochastic Modeling

Model verification: synthetic single pattern simulations using seismic reflection data

Abelardo Ramirez[1], Kathleen Dyer[1], Donald White[2], Yue Hao[1],
Xianjin Yang[1]

1-Lawrence Livermore National Laboratory
2-Geological Survey of Canada

LLNL-TR-441596

Abstract

During Phase 1 of the Weyburn Project (2000-2004), 4D reflection seismic data were used to map CO_2 migration within the Midale reservoir, while an extensive fluid sampling program documented the geochemical evolution triggered by CO_2-brine-oil-mineral interactions. The aim of this task (3b.11) is to exploit these existing seismic and geochemical data sets, augmented by CO_2/H_2O injection and HC/H_2O production data toward optimizing the reservoir model and thereby improving site characterization and dependent predictions of long-term CO_2 storage in the Weyburn-Midale reservoir.

Our current project activities have concentrated on completing and testing a stochastic inversion method that will identify reservoir models that optimize agreement between the observed and predicted seismic response. This report describes the results of a validation test that uses synthetic seismic data to identify optimal porosity/permeability distributions within the reservoir. The report partially fulfills deliverable D3: "Model verification: synthetic single pattern simulations" in the project's statement of work. A future deliverable will describe verification activities related to the geochemical inversion algorithm.

Introduction

When completed, our completed stochastic inversion tool will explicitly integrate reactive transport modeling, facies-based geostatistical methods, and a novel stochastic inversion technique to optimize agreement between observed and predicted storage performance. Such optimization will be accomplished through stepwise refinement of: 1) the reservoir model—principally its permeability magnitude and heterogeneity—and 2) geochemical parameters—primarily key mineral volume fractions and kinetic data. We

anticipate that these refinements will facilitate significantly improved history matching and forward modeling of CO_2 storage. Our tool uses the Markov Chain Monte Carlo (MCMC) methodology.

Deliverable D1, previously submitted as a report titled "Development of a Stochastic Inversion Tool To Optimize Agreement Between The Observed And Predicted Seismic Response To CO_2 Injection/Migration in the Weyburn-Midale Project" (Ramirez et al., 2009), described the stochastic inversion approach that will identify reservoir models that optimize agreement between the observed and predicted seismic response. The software that implements this approach has been completed and requires that its performance be verified.

This document contains deliverable D3, a report that summarizes verification activities that evaluate the performance of the software and its ability to recover reservoir model permeabilities that optimize agreement between measured and predicted seismic reflection data. A future deliverable will describe verification activities that ensure recovery of geochemical parameters (mineral volume fraction, kinetic parameters) that optimize agreement between measured and predicted aqueous chemistry data.

Testing approach

Introduction

The software validation approach we followed consisted of the following steps. First, we generated random realizations of porosity/permeability. In this document, we call these realizations reservoir models. These models honored geostatistical trends in Cenovus' model calibrated against several decades of production data. Realizations also honored lithology designations and layer boundariesin Cenovus' model.

We then arbitrarily selected one of these reservoir models as the "true" model. The next step was to run the flow simulator while honoring the CO_2 injection and fluid production rates used in the field; this step predicted various reservoir parameters such as fluid densities, CO_2 saturation and pore pressure. We then predicted seismic velocities throughout the model using the calculated reservoir parameters and Gassmann's equation (see Ramirez et al., 2009, for details). The velocity model was then used to compute seismic reflectivities and and zero-offset, 1D seismograms. The seismograms became the "observed data" used by the stochastic inversion to find the optimal permeability models. We then ran the MCMC inversion software to find those permeability models that best fit the seismic data. The permeabilities recovered by the inversion were then compared to the "true" model to assess their similarity.

Figures 1 and 2 show details of the reservoir region assumed for the test. The region consisted of pattern 16 (location shown in Figure 2) and included a CO_2 injector, oil producers and water injectors as shown in Figure 1. The size of the region is 1.17 km by 1.17 kilometers by 1.46 km.

The reservoir models honor information contained by Cenovus' lithology/permeability model. Their model has been calibrated against production data collected over a period of decades. Our realizations honor their lithology designations and layer boundaries. The realizations allow porosity and permeability to vary spatially between each layer while honoring the porosity/permeability trends embedded in their model (Figures 3 and 4). The porosities come from the bimodal distribution shown by the histogram in Figure 3, left side. The permeabilities come from the distribution shown on the right side of Figure 3. The porosity/permeability distributions also honor the cross-correlation trends shown in Figure 4.

We used the algorithm that generates the porosity/permeability realizations to generate a number of realizations. Ramirez et al. (2009) describe the algorithms we use for this process in detail. One of these reservoir models was arbitrarily chosen to be the "true" model and is shown by the lower row of images in Figure 5. These images show horizontal slices through the model, 6m above, 0 m, and 4 m below the location of the CO_2 injector. The flow simulator was then used to compute various reservoir parameters such as fluid density, pressure and CO_2 saturation needed to compute seismic velocity. The flow simulator used as input the "true" reservoir model as well as the injection/production volumes observed during field operations. The simulation assumed that water was injected for 2 years, and that CO_2 injection started after 0.7 years of water injection. The top row of images in Figure 5 show the CO_2 saturations calculated by the flow simulator after 1.3 years of CO_2 injection.

We then used an algorithm that implements Gassmann's equation to compute a seismic velocity model. Then the reflectivities within the reservoir were calculated and zero offset, 1D seismograms computed. These 1D seismograms became the "observations" used by the stochastic inversion to recover reservoir models that are consistent with the seismic data. We use the Monte Carlo Markov Chain (MCMC) stochastic inversion technique described in detail by Ramirez et al. (2009).

Results

Figures 6a and b show the current (last accepted) permeability model as a function of MCMC iteration. The horizontal slice shown is coplanar with the CO_2 injector. The top left images shows the "true" model. Note that after 70 iterations there are substantial similarities between the recovered image and the true model. Subsequent iterations show features that are qualitatively similar to the true model; however, the inversion values are somewhat higher than those in the true model. This is not surprising because the MCMC approach searches the space of possible solutions. It moves into a region were the models are very consistent with the observations and then, can move away in order to search for other (possible) regions that may be consistent with the observations. This means that the best models may not necessarily be at the end of a Markov chain (i.e., last iteration number) and thus, may be found at earlier iterations.

We now discuss models that best fit the "observed" zero-offset seismograms. We used the likelihood function values to identify these models. The likelihood function (see Ramirez et al., 2009 for details) provides a metric that indicates how similar are the predicted and observed seismic data for a given reservoir model realization.

Using this metric, we identified the top three models in a Markov chain that was 1100 iterations long. These models are shown in Figure 7. The left column of images shows three horizontal slices through the true permeability model, and the location of the CO_2 injector and oil producers. The remaining 3 columns of images show slices through reservoir models that exhibit the best likelihoods.

The inversion models are reasonably close to the true model. The slices coplanar with the CO_2 injector and oil producers (middle row of images in Figure 7) show regions of relatively high and relatively low permeabilities. Note the relatively high permeability zone located on the lower left quadrant of the true model is matched reasonably well by high permeability zones in the inversion models
The slices at 6m above the CO_2 injector (top row of images, Fig. 7) are similar to the "true" model and all show regions with relatively high permeability. Similar comments can be made on the slices located 4 m below the injector well (bottom row of images).

It is well known that inversions of geophysical data are typically non-unique and the solution(s) are uncertain. One of the strengths of our stochastic inversion method is that it provides the information needed to characterize solution uncertainty. The differences between the inversion models in Figure 7 are indicative of the uncertainty associated with the inversion results. Image features that are similar in all inversion models indicate a higher level of confidence that the features represent the true model. Conversely, features that vary from one inversion to the next are associated with a higher level of uncertainty and therefore, we are less confident that they are representative of the true model. We are currently developing tools that can be used to rigorously characterize solution uncertainty. These will be discussed in future deliverables.

One interesting aspect of these results is that the inverted models appear to recover reasonable permeabilities in regions not invaded by the CO_2 plume. Consider the extent of the CO_2 plume shown by the top row of images in Figure 5, particularly in the slice coplanar with the CO_2 injector (top row, middle image). Note that the plume extends to the locations of the oil producers closest to the CO_2 injector. Now consider the high permeability zone in Figure 7 (middle row of images) located in the lower left quadrant of each image. The CO_2 plume does not invade this region of higher permeability and yet, the inversion recovers permeabilities that are reasonably close to the true model. We know that the pressure field in the reservoir is affected by the permeability distribution and the rock and fluid bulk moduli are pressure sensitive. This means that pressure changes caused by injection/extraction can cause seismic velocity changes that can be detected. Laboratory measurements made on reservoir core by Brown (2002) corroborate this assertion.

We propose that pressure fluctuations caused seismic velocity changes that affected the "observed" seismograms, thereby providing sensitivity to reservoir permeability in regions affected by the pressure pulse. To test this hypothesis, we conducted a numerical experiment where we predicted the reservoir conditions and associated P velocities for two scenarios. In scenario 1, no CO_2 injection or fluid extraction was allowed. The seismic velocities associated with this case (let's call this velocity model V1) were calculated using the process described earlier in this report. For the second scenario, we allowed CO_2 injection and extraction over a 1.3 year period. Let's call the velocity model predicted for this case, V2. We then calculated the P velocity changes (V1 – V2) and analyzed the results.

Figure 8 summarizes the results of this simulation. The left column of images shows the "true" permeability model used by the flow simulator. The second and third image columns show the calculated pressure and CO_2 saturation that develop after 1.3 years of CO_2 injection. The fourth image column shows the changes in P velocity (V1 – V2). Note that the P velocity decreases around the CO_2 injection well as expected by as much as 100 m/s. Now look at the velocity changes within the white ellipse where the velocity decreases a smaller amount, about 35 m/s. Note that the white ellipse does not intercept the region where the CO_2 plume is located. This suggests that the capacity to recover permeabilities in this region is due to the changes in velocities caused by pressure changes. The changes caused by the CO_2 plume are about 3 times larger than those created by pressure effects. This analysis suggests that the seismic data is primarily sensitive to CO_2 saturation and, to a lesser extent, to the pressure perturbations associated with the injection/extraction process.

Computational Expense
Perhaps the greatest challenge associated with the use of our stochastic inversion approach is its computational expense. Almost all the expense is in running the flow simulator that predicts reservoir conditions caused by injection/extraction operations. The number of realizations required for the Markov chains to reach convergence is expected to be 2000 – 6000.

Our initial algorithm implementation would have required between 16 and 48 days of wall clock time to reach convergence for just one reservoir pattern (like the validation test described previously). For a multi-pattern test, the required time would increase substantially. Clearly, these run times needed to be reduced substantially to make the technique useful.

We spent a considerable amount of effort in modifying/testing the initial implementation to increase its time efficiency. After these modifications were implemented, the time required to reach convergence was reduced to a few days. These modifications include various multi-threading approaches described next.

Figure 9 schematically shows the nested, parallel-thread approaches implemented to date. Each Markov chain runs on a separate thread (left side of Figure 9). Then, each Markov chain thread is sub-divided by creating multiple reservoir realizations; Each realization is created by perturbing the last model that accepted by the MCMC algorithm and is run on a separate thread (see middle diagram in Figure 9). All these threads are further subdivided when the flow simulator is used because it runs in parallel mode. The combined effect of these modifications produced about a factor of 8 performance improvement. The number of processing cores used for the test was 104.

Summary
We have conducted a test of our stochastic inversion approach using synthetic, zero offset seismic data to recover the permeability distribution in the reservoir. We have identified reservoir models that best fit the "observed" seismic data and compared them to the "true" reservoir model. These comparisons suggest that the inversion is finding models that are reasonably close to the "truth". There is reasonably close agreement in the location of high and low permeability zones. Also, the permeability magnitudes are in reasonable agreement.

One somewhat surprising result is that the inversion models appear to recover a reasonable representation of the permeability field in regions not invaded by the CO_2 plume. We suggest that the capacity to recover permeabilities in this region is due to the changes in seismic velocities caused by pressure changes. The inversion results suggest that the seismic data is primarily sensitive to CO_2 saturation and, to a lesser extent, to the pressure perturbations associated with the injection/extraction process.

References
Brown, L. 2002, *Integration of rock physics and reservoir simulation for the interpretation of time-lapse seismic data at Weyburn Field, Saskatchewan*, M. Sc. thesis, Colorado School of Mines, Golden, CO.

Ramirez, A., Y. Hao, D. White, S. Carle, K. Dyer, X. Yang, W. Mcnab, W. Foxall, and J. Johnson, 2009, *Development of a Stochastic Inversion Tool To Optimize Agreement*

Between The Observed And Predicted Seismic Response To CO_2 Injection/Migration in the Weyburn-Midale Project, Lawrence Livermore National Laboratory, LLNL-TR-420989, Livermore CA.
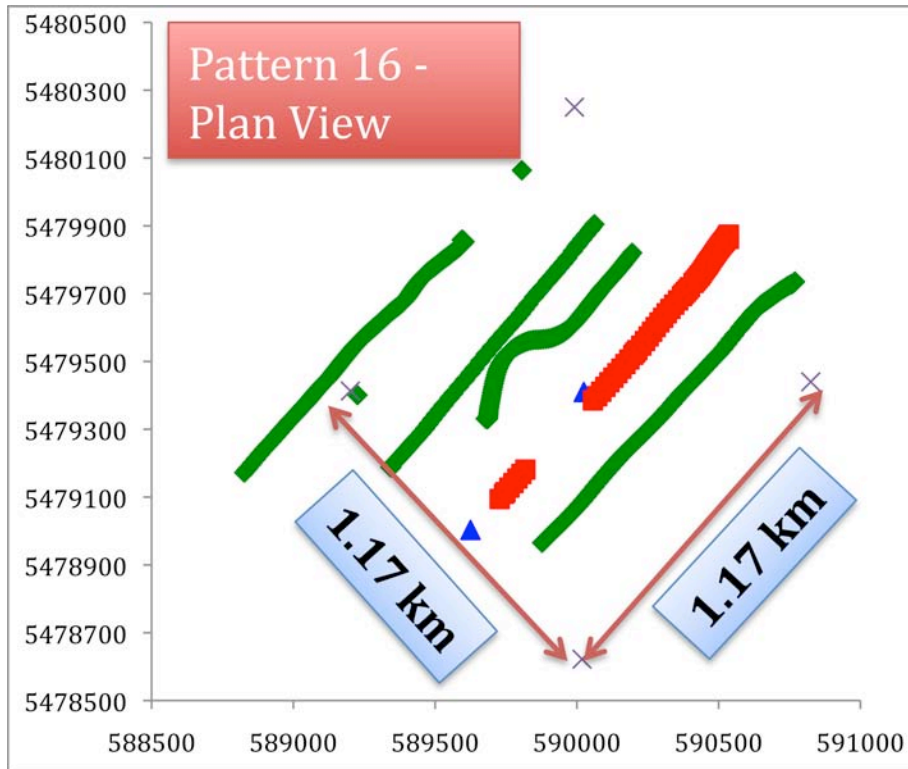

Figure 1 shows the well layout within the pattern of interest. The green segments represent the oil producers, the blue triangles represent the water injectors and the red segment represents the CO_2 injector.
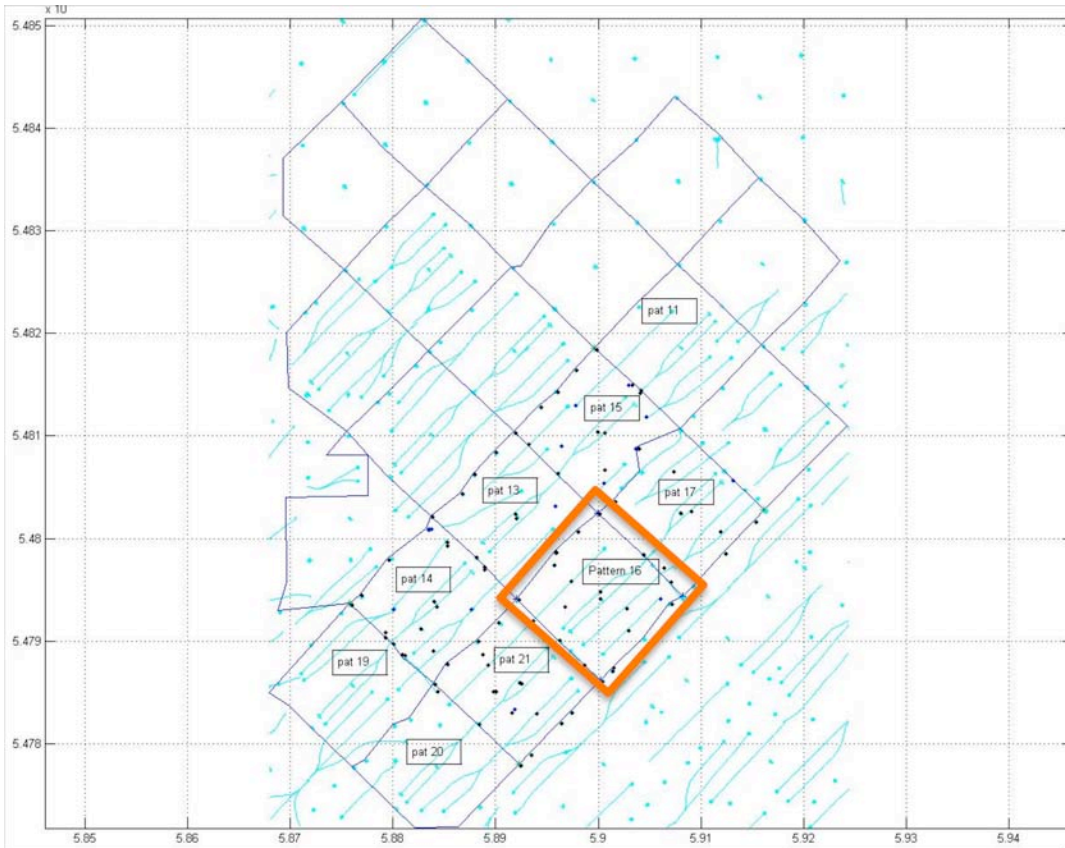
Figure 2. The red square shows the location of the pattern considered by the synthetic test, within the Phase 1A area of the Weyburn-Midale reservoir.
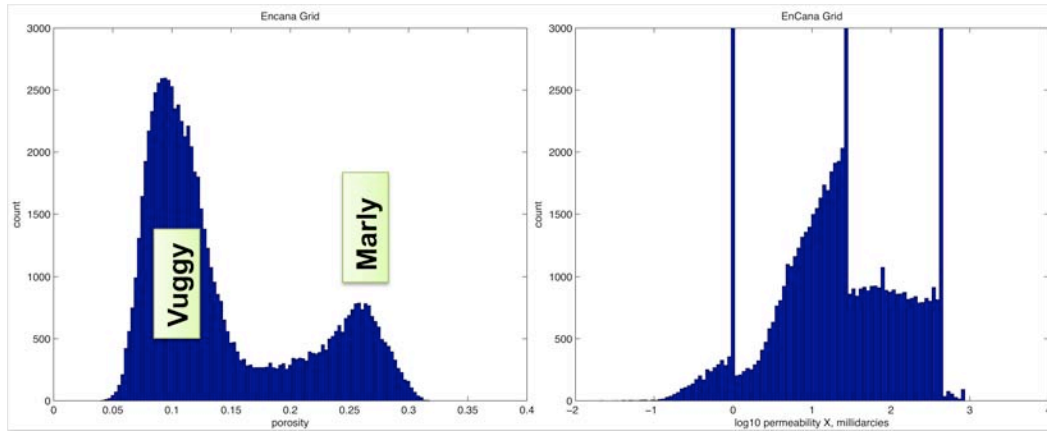
Figure 3. Histograms of porosity and permeability in Cenovus' model, calibrated against production and injection history.
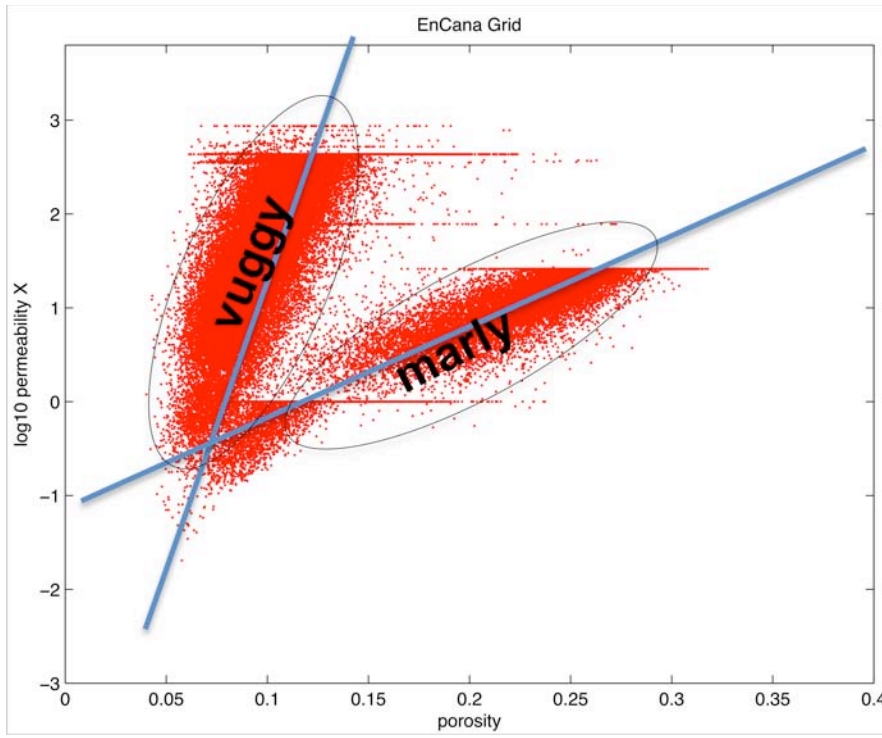
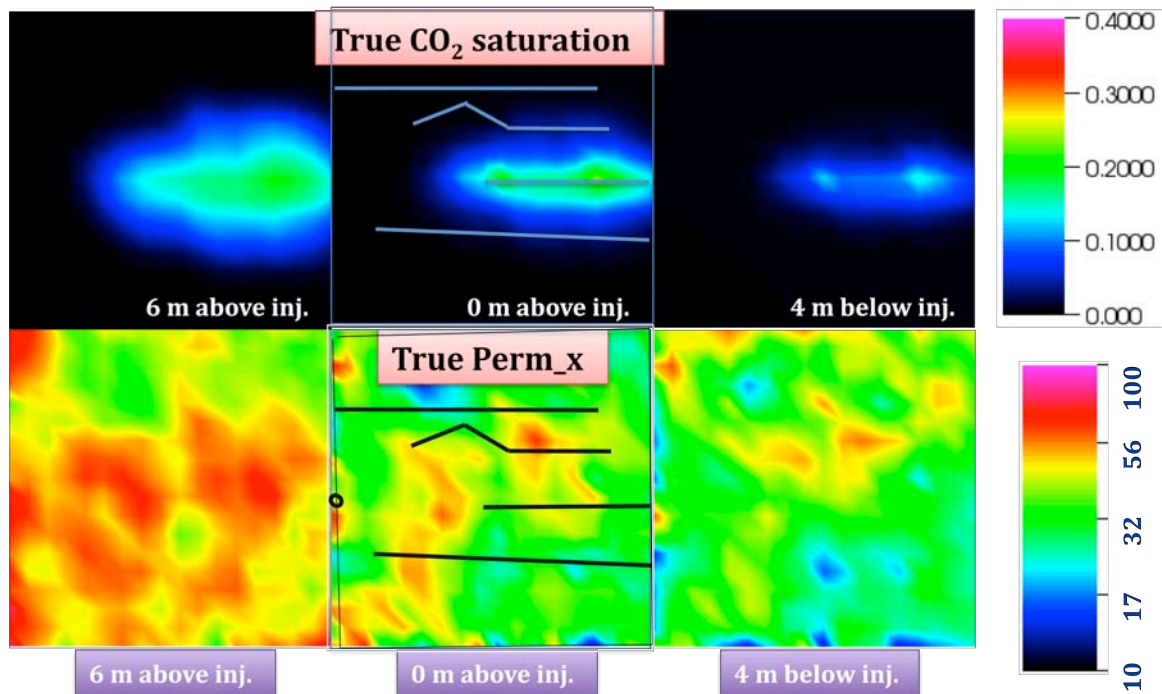Figure 4. Cross-plot of porosity versus permeability (inferred from Cenovus' model).

Figure 5. The top row of images shows the CO_2 distribution calculated assuming the permeability distribution in the bottom row of images. The image planes are horizontal and located at the elevation of the CO_2 injector, 6m above the injector and 4 m below the injector. The CO_2 saturation color bar is at the top right corner of the image. The permeabilities are in millidarcies (bottom right color bar).
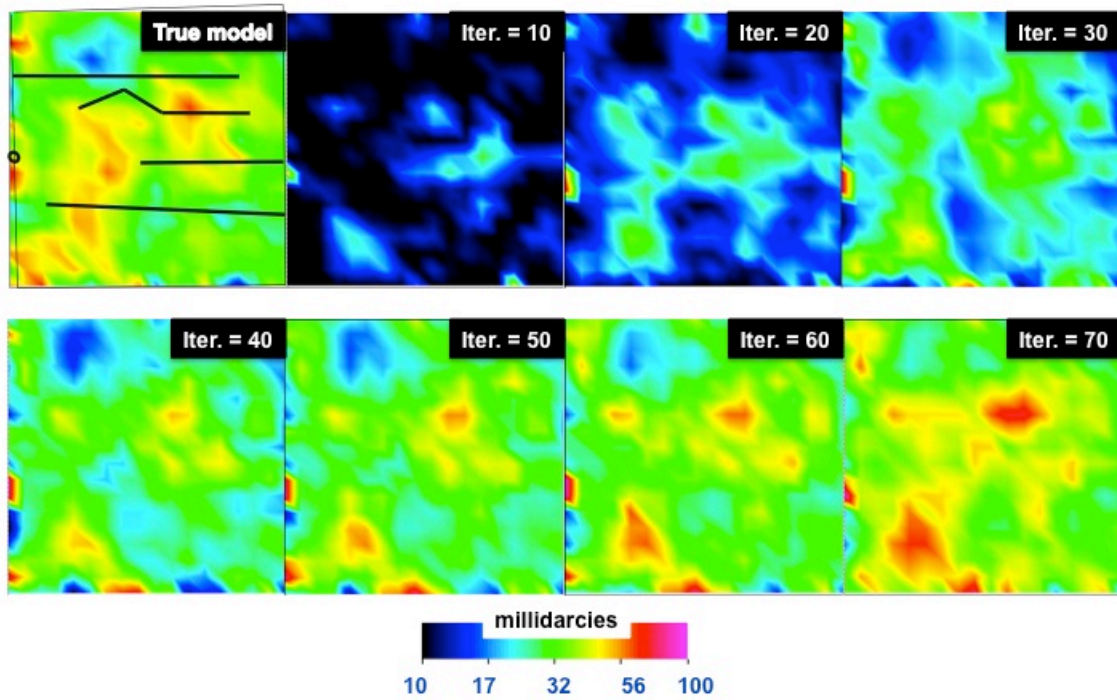
Figure 6a. The top left image shows the true permeability distribution and the locations of the CO_2 injector, oil producers and water injectors. The CO_2 injector is coplanar with the horizontal image plane shown. The remaining images show the recovered permeabilities as a function of MCMC iteration.
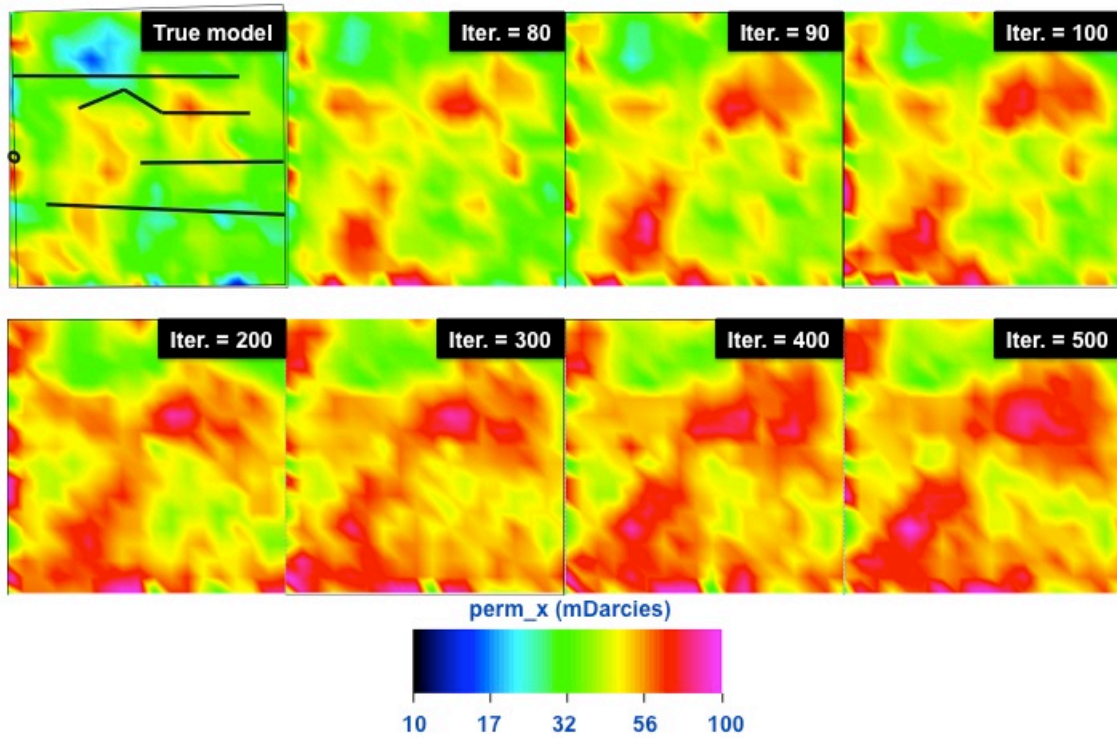
Figure 6b. The top left image shows the true permeability distribution and the locations of the CO$_2$ injector, oil producers and water injectors. The CO$_2$ injector is coplanar with the image plane shown. The remaining images show the recovered permeabilities as a function of MCMC iteration.
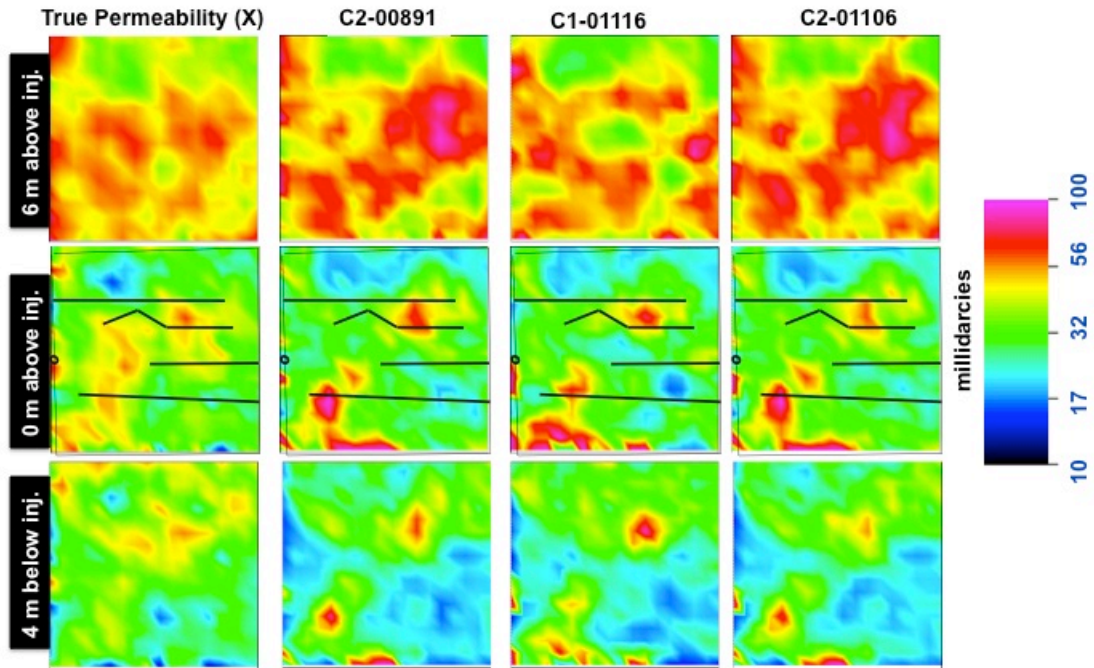
Figure 7. The left column of images shows horizontal slices through the true permeability model. The next three columns show recovered permeability distributions that best fit the synthetic seismic data.
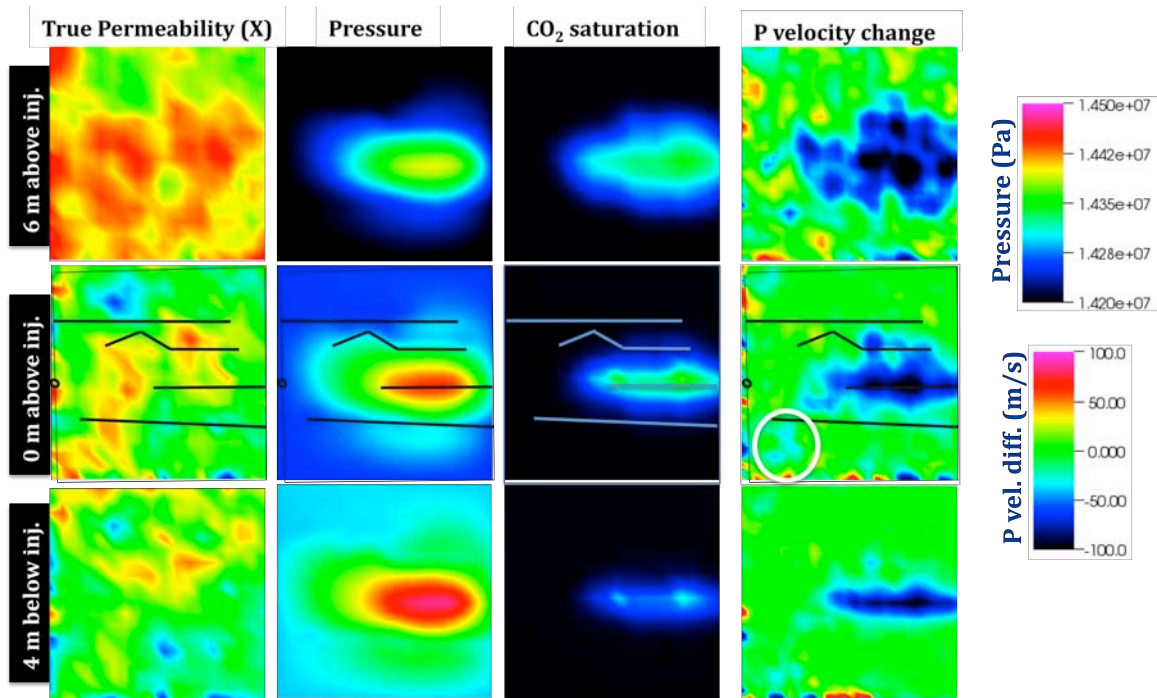
Figure 8. The left column of images shows the "true" permeability model. The second and third image columns show the calculated pressure and CO_2 saturation that develop after 1.3 years of CO_2 injection. The fourth image column shows changes in P velocity (V1 – V2) predicted, where V1 = velocity at ambient pressure and no CO2, and V2 = velocity at injection pressures and CO_2 saturations. The velocity changes within the white ellipse region are likely caused by pressure fluctuations created by the injection/extraction process.
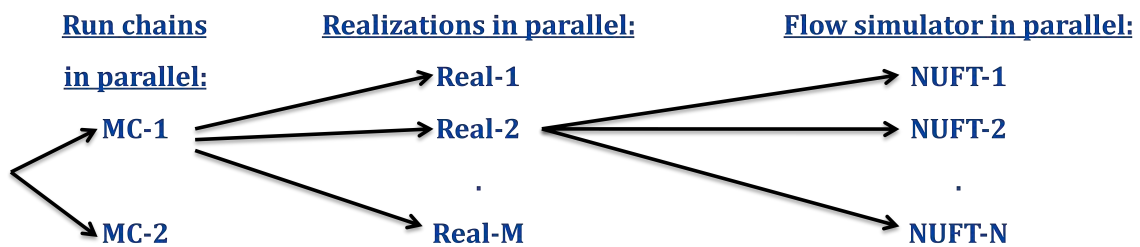

Figure 9 shows schematic implementation of the nested, parallel-thread approaches used to optimize run-time performance.